ADVANCED FUNCTIONAL MATERIALS
www.afm-journal.de

Materials Views
www.MaterialsViews.com

Piezoresistive Properties of Ag/Silica Nano-Composite Thin Films Close to the Percolation Threshold

T. Das Gupta, T. Gacoin, and A. C. H. Rowe**

The effect of mechanical stress on the electrical properties of Ag/silica nano-composite sol–gel films, fabricated using an ultra-violet (UV) photo-reduction process, is studied over a large range of Ag volume fractions, ϕ. The ability to finely tune ϕ in situ by varying the UV exposure time enables the direct identification of the critical volume fraction, $\phi^* \approx 13.1\%$, around which the resistance changes by 6 orders of magnitude and the average piezoresistive gage factor, $\langle G \rangle$, peaks at 4330. $\langle G \rangle$ is orders of magnitude larger than that of bulk silicon and ϕ^* is close to the value expected for percolation in 3 dimensions. It is shown experimentally that this giant piezoresistance is the result of a stress-induced change in the average Ag cluster size that significantly modifies the sample resistance when $\phi \sim \phi^*$. In terms of the potential use of any composite material as a sensitive strain sensor, a sensor figure-of-merit (F) that accounts for both $\langle G \rangle$ and for the measured, expected divergence in resistance fluctuations close to ϕ^* is defined. It is shown that maximum F is achieved in composites slightly to the metallic side of the percolation transition. In the case studied here, the maximum value of F, which is 5–10 times larger than that measured on commercial strain gages under the same conditions, is obtained for $\phi \approx 13.4\%$. The ability to finely tune ϕ in-situ therefore suggests that Ag/silica nano-composites could be the basis for a highly sensitive, low power, strain sensing technology.

1. Introduction

Conducting composite materials consist of a total volume, V_c, of conducting particles distributed throughout an insulating matrix of volume V_m. The electrical resistance as a function of the conducting volume fraction, $\phi = V_c/(V_c + V_m)$, has been widely studied since it reveals a percolative metal-insulator transition at the critical volume fraction, ϕ^*.[1,2] During this transition the resistance, R_0, can vary by many orders of magnitude with changes in ϕ as small as a fraction of 1%.[3] In a composite with ϕ approximately equal to but slightly larger than ϕ^*, R_0 varies as:

$$R_0 \propto (\phi - \phi^*)^{-t} \tag{1}$$

where the parameter t is known as the critical scaling exponent. In a 3-dimensional random network of conducting spheres, the Scher and Zallen criterion[4] predicts $\phi^* \approx 15\%$ whereas t is expected to lie between 1.6 and 2 depending on the exact nature of the percolation.[5,6] Percolation theory not only quantitatively describes the observed resistance variations with changes in ϕ near ϕ^*, but is highly intuitive; increases in ϕ correspond to an increase in the average size of the randomly distributed conducting clusters. When the average cluster size is equal to the sample size, the composite undergoes the percolation transition. Near ϕ^* therefore, any external perturbation that modifies the average cluster size will significantly modify the resistance.

One such force is mechanical stress, and resistance changes of several orders of magnitude have been observed with biaxial strains of several percent in elastomer based carbon black composites.[7] Strains of several percent under hydrostatic pressure[7–9] or uniaxial stress[10–12] have also been observed to significantly modify the electrical resistance of composites. Consequently composite materials near the percolation threshold are now widely recognized as being of potential interest as sensitive strain gages because they may exhibit a so-called giant piezoresistance.[13–19] Piezoresistance is defined as the resistance change induced by an applied mechanical stress, and its magnitude is quantified by the gage factor, G, defined as the relative resistance change per unit strain (ε):

$$G = \frac{\Delta R}{R_0}\frac{1}{\varepsilon} = \frac{1}{R_0}\frac{\mathrm{d}R}{\mathrm{d}\varepsilon} \tag{2}$$

where R is the resistance under applied stress and R_0 is the reference (or zero-stress) resistance. In addition to a simple change of sample geometry or cluster size, applied stress can also modify the electronic structure and thus the electrical resistivity of solids. This has been studied widely in silicon[20] where $G \approx 100$, and in metals[21] where $G \approx 2$. Indeed these materials are today used as strain gage transducers for a range of applications[22,23] and there are efforts underway to increase G via reductions in size.[24,25]

The literature on conducting composites deals generally with physical mixtures of insulating particles and particles of either a

T. D. Gupta, Dr. T. Gacoin, Dr. A. C. H. Rowe
Physique de la matière condense
Ecole Polytechnique
CNRS, Route de Saclay, 91128 Palaiseau, France
E-mail: thierry.gacoin@polytechnique.edu;
alistair.rowe@polytechnique.edu

DOI: 10.1002/adfm.201303775

© 2014 WILEY-VCH Verlag GmbH & Co. KGaA, Weinheim

carbon allotropes[3,7,9,11,13–15,17,19] or metallic particles.[8,10,12,16,18] Once mixed, the relative volumes of the two components determine a value for ϕ which cannot be subsequently modified. This pre-determined mixing of components limits the scope of experimental studies because each value of ϕ requires a different sample. Moreover, since the critical region where percolation occurs corresponds to a narrow range of ϕ, it is difficult with pre-mixed composites to correctly target ϕ^* since its exact value depends sensitively on the spatial distribution and aspect ratio of the conducting particles.[6] Consequently, while G is expected to diverge to very large values near ϕ^* (see below), it is difficult to find cases in the literature where G is significantly larger than 100.

Here we explore the percolative piezoresistive properties of an Ag/silica nanocomposite thin films in which Silver nanoparticles are produced in-situ through a TiO_2 mediated photocatalytic reduction of ionic silver into the host porous silica matrix. This original approach permits an in situ variation of ϕ within the same sample, merely by varying the exposure time to an ultra-violet (UV) light source. Moreover, ϕ can be finely tuned in this way near the percolation threshold, facilitating access to the physical properties of the material very close to ϕ^*. In this way gage factors of more than 4000 are measured close to ϕ^*, significantly larger than those reported in other works. Importantly, this fine tuning capability enables new insight into the applicability of any composite material as a strain gage. Experimentally, resistance fluctuations are found to diverge close to ϕ^* as expected, and consequently the use of composites too close to the percolation threshold is not recommended. By defining a figure of merit that accounts both for G and for the resistance fluctuations it is shown experimentally and theoretically that the optimal conducting volume fraction is slightly to the conducting side of the percolation threshold since this maximizes G while minimizing resistance fluctuations.

2. Sample Fabrication and Zero-Stress Electrical Properties

The fabrication of Ag/silica nano-composite thin films was recently developed in our laboratory.[26] This process, based on the photo-catalytic reduction of Ag^+ ions using TiO_2 nanoparticles as the photo-catalyst inside a porous matrix, permits a continuous and fine tuning of the Ag volume fraction up to 18% by varying the exposure time to a UV light source during synthesis. UV photo-reduction of Ag takes place while the sample is immersed in a 0.05 M $AgNO_3$:isopropanol (1:1 volume ratio) solution, leading to the formation of metallic Ag clusters within the pores of the insulating, active silica layer only. Increasing UV exposure time generates new metallic silver nanoparticles randomly throughout the silica matrix which may, or may not, be in contact with existing silver clusters. The probability that new nanoparticles will be spatially isolated from existing clusters decreases as the metallic volume fraction increases. In this way, increasing UV exposure times increase the average metallic silver cluster size. According to standard percolation theory, when the average cluster size reaches the sample size, the material undergoes a percolative insulator-to-metal transition. Indeed, a study of the resistance of Ag/silica nanocomposites as a function of temperature at large ϕ reveals metallic behavior indicating that with increasing ϕ, Ag/silica nano-composites undergo an insulator to metal transition as expected.[26]

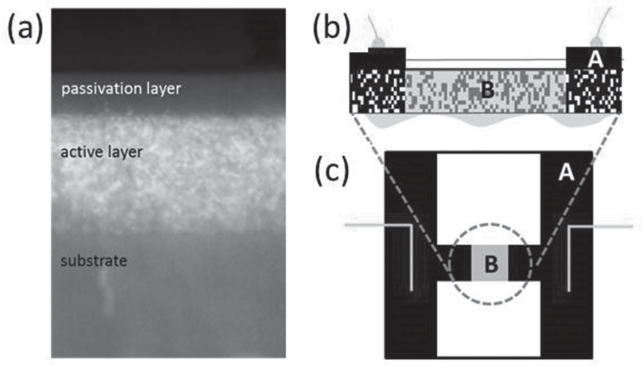

Figure 1. a) Cross-sectional SEM image showing the active layer containing Ag clusters (white) in a porous silica matrix, and the passivation layer consisting of the porous silica matrix only. b) A schematic side view of the contacted Ag/silica nano-composite. The black regions represented by A correspond to the fully exposed electrical contacts, whereas the light region denoted by B corresponds to the active area of the film. The dark gray dots in region B represent silver clusters whereas the light brown region corresponds to the insulating silica matrix. The white layer on the top of region B represents the porous silica passivation layer. c) Schematic diagram showing the top view of the sample with the active area (B) between the two fully exposed contacts (A). External leads for the resistance measurement are shown in yellow.

Figure 1a shows a scanning electron microscope side view of a sample which, before photo-reduction of the Silver ions, consists of two layers; an active layer spin-coated directly onto a glass substrate consisting of a 450 nm thick, porous silica film containing TiO_2 (titania) nanoparticles, and a 150 nm thick porous silica passivation layer. The passivation layer improves the homogeneity of the Ag deposit by confining it to the active layer without blocking the formation of Ohmic contacts to the active layer.[2,26] In order to fabricate Ohmically contacted samples the bilayer coating is first masked using Kapton so that the unmasked parts can be maximally loaded with Ag ($\phi \approx 18\%$) by exposing the solution and sample to a 1 mW cm^{-2}, 312 nm light source for 50 min (total photon exposure $\approx 10^{18}$). In this way, the two contact areas (denoted by A) in Figure 1b and the vertical arms of the 'H' structures in **Figure** 1c,2a (top view) are formed. These areas are then connected to external wires (Figure 1b,2b) using conductive silver paint. All unexposed parts of the coating are then mechanically removed except for a central square (labeled B in Figure 1,2) of dimension 5 mm × 5 mm between the two black electrodes. This constitutes the active area whose electrical properties are to be measured (light brown area in Figure 1c,2b). For a given UV exposure time, ϕ is determined by taking images of the sample (see Figure 2a) from which the gray-level or brightness is quantified. This is then related to the absorbance of equivalent films on transparent glass substrates from which ϕ can be estimated.[26] Details of the calibration procedure are given in the Supporting Information.

The electrical measurement is carried out using a voltage source and a pico-ammeter so that the resistance can be measured as shown in Figure 2b. Note that a two probe resistance

© 2014 WILEY-VCH Verlag GmbH & Co. KGaA, Weinheim

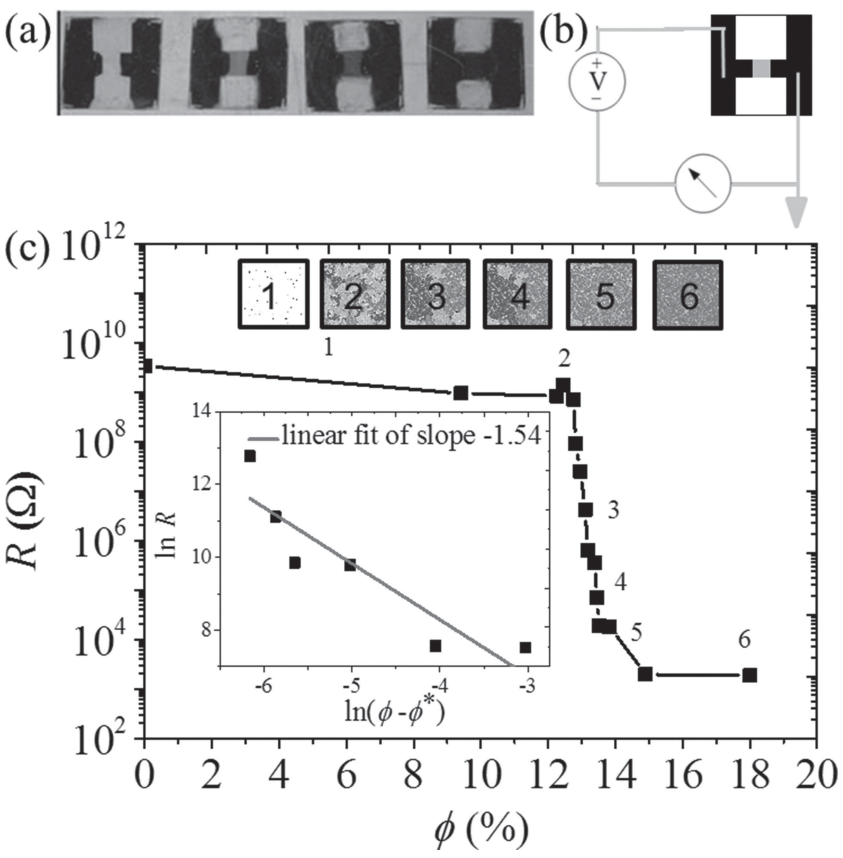

Figure 2. a) Top view of the sample after (from left to right) 0 s, 90 s, 100 s, and 120 s exposure to a 3.5 mW cm^{-2}, 312 nm source. The black areas are the fully pre-exposed electrical contacts while the central active area progressively darkens as ϕ increases with increasing exposure time. Analysis of the sample color is used to determine ϕ. b) Schematic diagram of the electrical connections used to measure R. c) The variation in R_0 with ϕ showing a rapid decrease by 6 orders of magnitude around $\phi = 13\%$. Determination of ϕ^* from the peak value of G (see Figure 3) permits the estimation of $t = -1.54$ in Equation 1 (see inset). The shaded areas in the colored areas in the schematic diagrams indicate individual Ag clusters, the average size of which increases with increasing ϕ. The largest Ag cluster at each stage is shown in red. Average cluster size increases gradually through the insulating region (diagrams 1–4). Diagrams 3–5 correspond to the transition region where average cluster size increases rapidly until it reaches the active area size (diagram 5). This corresponds to ϕ^*. Diagram 6 corresponds to the metallic side of the transition where a single Ag cluster exists.

measurement is found to be sufficient since the contact resistances are negligible compared to the active area resistance at maximum ϕ despite the presence of the passivation layer. A single sample is measured over the full range of ϕ by progressively increasing the cumulative UV exposure time so that R_0 and G can be measured for a discrete number of well-defined ϕ values.

The dependence of R_0 on ϕ shown in Figure 2c shows a very sharp transition (points 3, 4, and 5) from a highly resistive region (points 1 and 2) to a conducting region (point 6) for ϕ between 12.5% and 13.5%. Note that the ability to finely tune ϕ permits multiple points to be measured in the transition region which is important for the following discussion. The transition region covers a range of ϕ that includes critical volume fraction, ϕ^*, at which percolation occurs. The usual procedure to determine both ϕ^* and t in Equation 1 is via a two-parameter curve fit of the continuously varying R_0 versus ϕ curve of Figure 2c. Depending on the values one obtains, the identification of a percolative phase transition is possible. However, as discussed below a direct determination of ϕ^* is possible via a measurement of G which then leaves t to be determined from a single parameter fit to the R_0 versus ϕ curve. In this way more accurate values ϕ^* and t are obtained which significantly improves the identification of a percolation threshold.

3. Piezoresistive Behavior as a Function of ϕ

Consider an expansion of the expression for G in Equation 2 obtained using the chain rule,

$$G = \frac{1}{R_0}\frac{d\phi}{d\varepsilon} \times \frac{dR}{d\phi} \tag{3}$$

which shows that G is proportional to the first derivative of the R versus ϕ curve of Figure 2c. By definition, the critical volume fraction at which percolation occurs is the point of maximum slope of the R versus ϕ curve[6] and therefore the volume fraction at which G is maximized. An approximate expression for $d\phi/d\varepsilon$ in Equation 3 has been derived elsewhere[7] and G may then be written:

$$G \approx -\frac{\phi(1-\phi)}{R_0} \times \frac{dR}{d\phi} \tag{4}$$

which fully determines its expected variation with ϕ based on an experimental measurement of $R(\phi)$. From a theoretical percolation viewpoint, substitution of Equation 1 into Equation 4 gives an expression for G arising from percolative conduction near ϕ^*:

$$G \propto \phi(1-\phi)(\phi - \phi^*)^{-1} \tag{5}$$

While Equation 4 is valid for any value of ϕ, Equation 5 is valid only for ϕ close to and greater than ϕ^*. The latter equation shows that on the basis of percolation theory, G is not only maximized at ϕ^*, but is expected to diverge according to a power law of exponent −1.

Here G is measured under uni-axial strain applied parallel to the direction of current flow in the device (see **Figure 3**, insert with arrows representing the direction of the applied stress) using an original technique shown schematically in Figure 3 (top). The sample shown in Figure 2a,b is glued with cyanolit 202 in the middle of a rectangular steel plate (length = 50 cm, width = 5 cm and thickness, d = 0.6 mm). When subjected to compressive forces at its two ends as shown in Figure 3 (top),

© 2014 WILEY-VCH Verlag GmbH & Co. KGaA, Weinheim

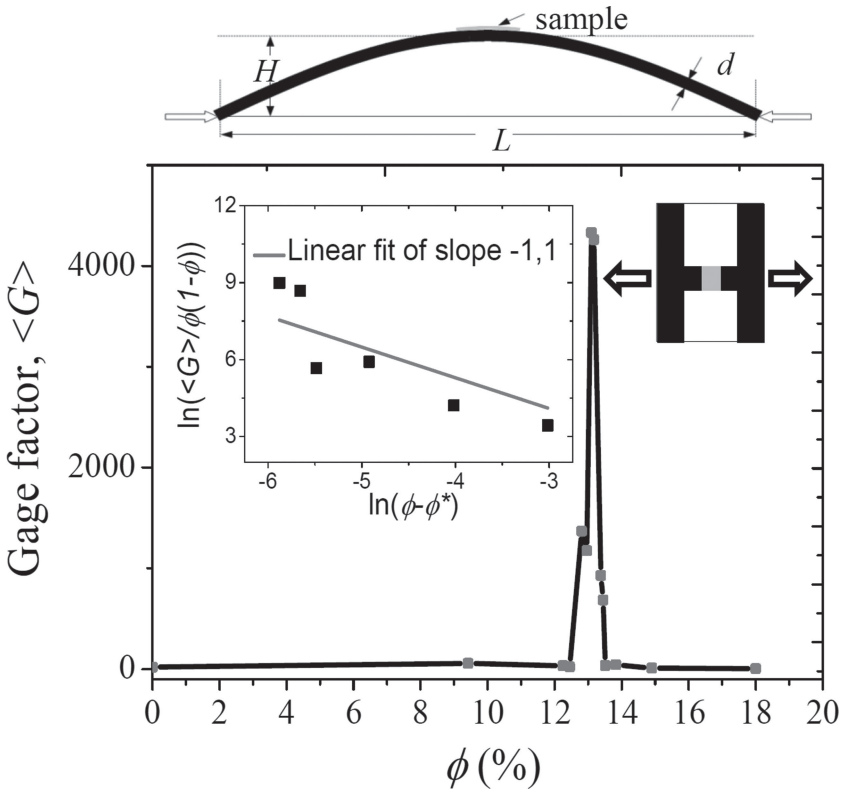

Figure 3. A side view of the apparatus used to apply the stress (top). The sample is glued onto a steel plate which is bent by a horizontal force applied to each end (arrows). Measurement of L and H, along with the plate thickness, d, is used to determine the uniaxial strain, ε, according to Equation 6. The applied stress is parallel to the direction of the current flow as indicated by the thick arrows on the schematic diagram (inset). The main figure shows the variation in $\langle G \rangle$ with ϕ. The peak in $\langle G \rangle$ (4300) occurs at $\phi^* = 13.1\%$. The inset shows ln [$\langle G \rangle/\phi(1-\phi)$] plotted against ln($\phi - \phi^*$), the slope of which is –1.1 which demonstrates that the gage factor diverges near ϕ^* according to the percolation theory based expression in Equation 5.

the plate deforms into a sinusoidal shape of half-wavelength L and amplitude H. If a sample of thickness comparable to d is glued to the top face of the plate, it experiences a uniaxial tensile strain, ε, given by (see Supporting Information)

$$\varepsilon = \frac{\pi^2}{2}\frac{dH}{L^2} \tag{6}$$

ε can therefore be determined by independently measuring L and H and through the use of Equation 6. In the experiment, the applied stress is modulated between two values in order to separate out resistance drift due to dielectric relaxation in the silica matrix from true piezoresistance.[25] In this way an average gage factor, $\langle G \rangle$, is obtained over several hundred independent measurements with $\varepsilon = 10^{-4}$ (see data in Figure 3). As shown in the Supporting Information, the resistance change is not linear in agreement with ε as has previously been observed in composite materials under mechanical stress.[7] While this will yield a value of $\langle G \rangle$ which depends on ε, it does not affect the following qualitative discussion. A clear cut and very sharp peak in $\langle G \rangle$ is observed with a maximum value (4330) well above that of reported values in other composite materials.[13–19] In other samples, values of up to ≈12 000 have been observed. Based on Equation 5, the peak occurs at $\phi = \phi^* \approx 13.1\%$, close to the ≈15% expected from the Scher and Zallen criterion for 3-dimensional site percolation in a randomly distributed network of spheres. [4]

The value for ϕ^* obtained in this way is used with the resistance data of Figure 2 to obtain the critical exponent t in Equation 1 via a single parameter fit, the result of which is shown in the inset of Figure 2. By plotting ln(R) versus ln(ϕ–ϕ^*) for ϕ close to but greater than ϕ^*, the slope yields $t \approx 1.54$ which is close to the theoretically expected range of possible values (1.6 to 2)[5,6] and within the range of experimentally measured values that have been associated with 3D percolation. A similar treatment can be applied to the experimental gage factor data. The inset of Figure 3 shows $\ln\{\langle G \rangle/[\phi(1-\phi)]\}$ plotted against ln(ϕ–ϕ^*), again for ϕ close to but greater than ϕ^* and here the slope is –1.1. This is very close to the value of –1 expected from Equation 5 when it is divided through by $\phi(1-\phi)$. The excellent agreement obtained here suggests that Equation 1 and Equation 6 are accurate descriptions of the resistance and gage factor dependence on ϕ respectively, and therefore that the Ag/silica nano-composites transit from an insulating phase to a metallic phase via a 3-dimensional percolation transition at ϕ^*. Moreover, this interpretation is reinforced when the zoomed $R(\phi)$ curve (**Figure 4**a) is numerically differentiated with respect to ϕ according to Equation 5 in order to obtain the curve shown in Figure 4b. The result is in excellent agreement with the experimentally measured variation of $\langle G \rangle$ with ϕ (the zoomed version of which is shown in Figure 4c).

Qualitatively therefore, the piezoresistive behavior of the nano-composite can be described as follows: in the strongly insulating phase ($\phi << \phi^*$) R_0 is large because the Ag clusters are small and disconnected (see the schematic figure labelled 1 in the inset of Figure 2). While strain in the sample changes the average cluster size by changing the connectivity between clusters, it does not change the electrical connectivity between the external Ohmic contacts because the clusters are always smaller than the sample size. The sample remains insulating regardless of the applied stress, $\langle G \rangle$ is small and conduction presumably occurs via tunneling or hopping processes between Ag clusters.[1] Increasing ϕ to the transition region corresponds to an increase in the average cluster size (see schematic figures labelled 2, 3 and 4 in Figure 2) up to the critical point, ϕ^*, where the average cluster size is equal to the sample size (see schematic figure labelled 5 in Figure 2). In this case straining the sample again changes both the average cluster size and the connectivity between clusters, but this then results in a change in the metallic connectivity between the external contacts. Applied stress can therefore significantly modify the sample resistance, $\langle G \rangle$ is large, and conduction occurs via percolative

© 2014 WILEY-VCH Verlag GmbH & Co. KGaA, Weinheim

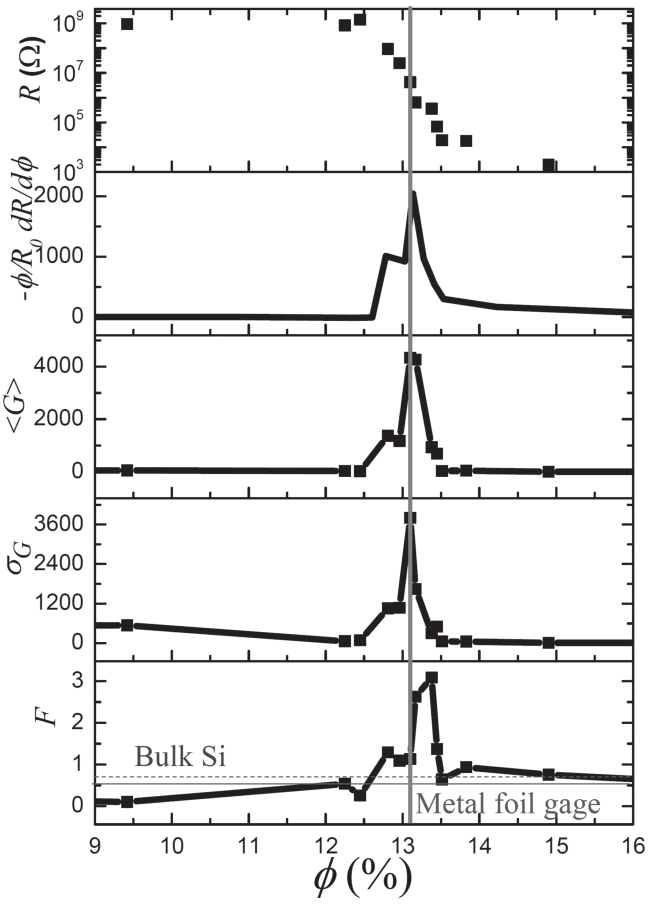

Figure 4. Plots of the variation of a) R, b) derivative calculated according to Equation 4, c) <G>, d) σ_G, and e) F with ϕ showing the position of ϕ^* (red, vertical line) for each quantity. When calculated from the derivative of R(ϕ) according to Equation 4, the resulting curve is in very good agreement with the measured, average gage factor, <G>. The fluctuations in G over multiple measurements (denoted σ_G) also show a sharp peak at ϕ^* as expected. With respect to the use of composite materials as strain gages, a figure-of-merit (F) defined in Equation 6 peaks at 5–10 times the value measured in bulk silicon (blue, dotted line) or in metallic foil gages (purple line), 0.3% to the metallic side of the percolation transition.

conducting paths in the composite. In effect, the mechanical stress sweeps the composite through the metal-insulator transition, similar to the situation observed in hybrid materials.[27] On the conducting side of the transition ($\phi >> \phi^*$), the sample consists of a single Ag cluster that remains connected to the external contacts even under stress so that both R_0 and <G> are small (see schematic figure labelled 6 in Figure 2). In this limit the composite behaves as a bulk metal.

4. The Figure of Merit for Composite Strain Gages

The literature already contains a number of studies concerned with the possible use of composite materials as strain gages for a variety of applications although none of them deal directly with materials over a wide range of ϕ from the fully insulating ($\phi << \phi^*$) to the fully conducting ($\phi >> \phi^*$) sides of the transition. Most importantly, aside from potentially large <G>, there is no discussion of the real utility of composite strain gages near ϕ^* where resistance fluctuations also diverge as $\phi \rightarrow \phi^*$ according to a power law.[28] This intrinsic variation in resistance can be due to several factors, for example temperature induced changes in the connectivity between clusters. Since R varies very rapidly with small changes in ϕ near ϕ^* the fluctuations are most apparent near the percolation threshold. Consequently, this yields a standard deviation over multiple measurements of the gage factor which varies according to

$$\sigma_G \propto (\phi - \phi^*)^{-k} \tag{7}$$

Depending on the origin of the fluctuation, k is expected to vary between 0.75 and 1.[28] This intrinsic variability in G means that nominally identical stresses will yield different piezoresistive responses if $\phi \sim \phi^*$. In terms of applications it is therefore necessary to define a figure-of-merit, F, that accounts for both the average value of the gage factor, <G> as well as its statistical variation, σ_G:

$$F = \langle G \rangle / \sigma_G. \tag{8}$$

F can be viewed as the intrinsic signal-to-noise ratio of any composite strain gage in the absence of external (extrinsic) noise sources. Note that while the experimental measurement is clearly not free of extrinsic noise sources, the noise power from these sources does not depend on ϕ. As such, the ϕ dependence of F which is of interest here, can be obtained from the experimental measurements. Moreover, by comparing the value of σ_G near ϕ^* with its value to either side of the transition in Figure 4d, the amplitude of the experimental noise can be estimated to be at most 1% of the amplitude of the intrinsic fluctuations. Figure 4d shows σ_G measured on the Ag/silica nano-composites as a function of ϕ. As expected it does indeed show a maximum at ϕ^*. σ_G is also found to obey a power law of exponent k = 0.97 (see Supporting Information), smaller than 1 and within the theoretically expected range. F can then be plotted as shown in Figure 4e, and there are a number of important points to note on this graph.

The first is that F is not maximized at ϕ^* but rather at ϕ^* + 0.3%, that is, slightly on the conducting, metallic side of the percolation threshold. The best way to use a composite as a strain gage is therefore to place it slightly above the percolation threshold and *not* at ϕ^* where <G> is maximized. Operation on the insulating side of the transition, or too far onto the metallic side of the transition results in significantly reduced values <G>,[13–19] while σ_G become very large too close to ϕ^*. The peak value of F measured here is 3, which is approximately 5 times higher than that measured in bulk silicon or in metallic strain gages under the same conditions (see respectively the dashed and solid horizontal lines in Figure 4e which were measured separately). The value of ϕ at which F is maximized is $\phi = \phi^*/k$ (see Supporting Information). Since theory[28] and measurement suggest $k < 1$, the maximum value of F should always be obtained for $\phi > \phi^*$ in any composite material. Using the measured values of k = 0.97 and ϕ^* = 13.1% yields ϕ = 13.4% for maximum F, in excellent agreement with the position of the measured peak in Figure 4e. Note also that for $\phi >> \phi^*$, F drops

© 2014 WILEY-VCH Verlag GmbH & Co. KGaA, Weinheim

to the solid line corresponding to a commercial metal foil gage, again indicating that the composite behaves simply as a bulk metal in this limit.

5. Conclusion

In summary, the percolative electrical properties of Ag/silica nano-composites have been explored in the presence of mechanical stress. Gage factors of over 4300 have been measured close to the critical Ag volume fraction $\phi^* = 13.1\%$. This giant piezoresistance makes composite materials potential candidates for ultra-sensitive strain gages as has been identified elsewhere. Here it is shown that because intrinsic fluctuations in G diverge at ϕ^*, use of any composite too close to the percolation threshold is not recommended. It is shown experimentally that the optimal Ag volume fraction lies less than 1% to the metallic, conducting side of ϕ^*. In this case a figure-of-merit for a nano-composite strain gage is shown to be 5–10 times larger than the equivalent in commercial strain gages. The optimal exploitation of composites as strain gages therefore requires the ability to finely control the metallic volume fraction near ϕ^* and, with respect to pre-mixed carbon-based and other composites studied elsewhere, this is a major advantage of the Ag/silica nano-composite presented here.

6. Experimental Section

Sample Preparation: Silica sol is prepared by using 11 mL of TetraEthylOrthoSilicate (TEOS), 11 mL of Ethanol (EtOH), and 4.5 mL of H_2O/HCl (pH ≈ 1.25). The solutions are mixed and heated for 1 h at a temperature of 60 °C. In the meantime, the solution of surfactant is prepared with a concentration that determines the porosity of the host silica matrix. In a typical experiment, 2.205 g of PE6800 (BASF) is mixed with 20 mL of EtOH on a hot water bath (60 °C) to increase dissolution kinetics. To this solution is added 10 mL of previously prepared silica sol. The whole mixture is then filtered using a 450 nm NYLON filter to remove eventual aggregates. 4 mL of the filtered mixture are mixed with 0.857 mL of a TiO_2 colloidal suspension (Crystal Global reference S5–300 A, 230 g L^{-1}) so that to have a Ti/Si ratio = 1. Film deposition (active and buffer layer successively) was achieved by spin coating onto a soda lime microscopy coverplate at a speed of 2000 rpm for 1 min. The substrates were previously cleaned using UV ozone for 15 min at 50 °C or by using piranha solution. After deposition of the first active layer, the sample is subjected to a humid atmosphere (65% humidity from saturated solution of magnesium acetate atmosphere) for 30 min so that to ensure appropriate condensation of the silica matrix. In a second step, the buffer layer is deposited using a sol of the same composition as for the active layer but without the TiO2 particles. After the deposition of the two layers, calcination of the samples is performed for 2 h at 450 °C to ensure the compete removal of the organic template.

Supporting Information

Supporting Information is available from the Wiley Online Library or from the author.

Received: November 7, 2013
Revised: February 19, 2014
Published online: April 14, 2014

[1] S. Kirkpatrick, *Rev. Mod. Phys.* **1973**, *45*, 574.
[2] L. N. Smith, C. J. Lobb, *Phys. Rev. B.* **1979**, *20*, 3653.
[3] S. Stankovich, D. A. Dikin, G. H. B. Dommett, K. M. Kohlhaas, E. J. Zimney, E. A. Stach, R. D. Piner, S. T. Nguyen, R. S. Ruoff, *Nature* **2006**, *442*, 282.
[4] H. Scher and R. Zallen, *J. Chem. Phys.* **1970**, *53*, 3759.
[5] A. L. Efros and B. I. Shklovskii, *Phys. Status Solidi B* **1976**, *76*, 475.
[6] D. Stauffer, *Introduction to Percolation Theory*, Taylor & Francis, London **1992**.
[7] F. Carmona, R. Canet, P. Delhaes, *J. Appl. Phys.* **1987**, *61*, 2550.
[8] D. Bloor, K. Donnelly, P. J. Hands, P. Laughlin, D. Lussey, *J. Phys D: Appl. Phys.* **2005**, *38*, 2851.
[9] J. F. Zhou, Y. H. Song, Q. Zheng, Q. Wu, M. Q. Zhang, *Carbon* **2008**, *46*, 679.
[10] J. E. Martin, R. A. Anderson, J. Odinek, D. Adolf, J. Williamson, *Phys. Rev. B.* **2003**, *67*, 094207.
[11] D. T. Beruto, M. Capurro, G. Marro, *Sens. Actuators A* **2005**, *117*, 301.
[12] G. Ausanio, A. C. Barone, C. Campana, V. Iannotti, C. Lupiano, G. P. Pepe, L. Lanotte, *Sens. Actuators A* **2006**, *127*, 56.
[13] M. Lillemose, L. Gammelgaard, J. Richter, E. V. Thomsen, A. Boisen, *Compos. Sci. Technol.* **2008**, *68*, 1831.
[14] M. Park, H. Kim, J. P. Youngblood, *Nanotechnology* **2008**, *19*, 055705.
[15] N. Hu, Y. Karube, M. Arai, T. Watanabe, C. Yan, Y. Li, Y. Lui, H. Fukunaga, *Carbon* **2010**, *48*, 680.
[16] C. Farcau, N. M. Sangeetha, H. Moreira, B. Viallet, J. Grisolia, D. Ciuculescu-Pradines, L. Ressier, *ACS Nano* **2011**, *5*, 7137.
[17] W. Yi, Y. Wang, G. Wang, X. Tao, *Polym. Test.* **2012**, *31*, 677.
[18] J. L. Tanner, D. Mousadakos, K. Giannakopoulos, E. Skotadis, D. Tsoukalas, *Nanotechnology* **2012**, *23*, 285501.
[19] J. Zhao, C. He, R. Yang, Z. Shi, M. Cheng, W. Yang, G. Xie, D. Wang, D. Shi, G. Zhang, *Appl. Phys. Lett.* **2012**, *101*, 063112.
[20] C. S. Smith, *Phys. Rev.* **1954**, *94*, 42.
[21] P. Bridgman, *Proc. Am. Acad. Arts Sci.* **1917**, *52*, 573.
[22] R. L. Hannah, *Strain Gage Users' Handbook,* S. E. Reed, Springer **1992**.
[23] S. P. Olson, *Patterned piezoresistive silicon strain gauge devices for use in low power applications* Proquest, Ann Arbor, MI **2008.**
[24] R. He, P. Yang, *Nat. Nanotechnol.* **2006**, *1*, 42.
[25] J. S. Milne, A. C. H. Rowe, S. Arscott, Ch. Renner, *Phys. Rev. Lett.* **2010**, *105*, 226802.
[26] J. Corde, S. Perruchas, L. Vieille, J.-P. Galaup, S. Duluard, C. Biver, J.-P. Boilot, T. Gacoin, *Nanotechnology* **2012**, *23*, 505206.
[27] A. C. H. Rowe, A. Donoso-Barrera, Ch. Renner, S. Arscott, *Phys. Rev. Lett.* **2008**, *100*, 145501.
[28] M. B. Heaney, *Phys. Rev. B* **1995**, *52*, 12477.

© 2014 WILEY-VCH Verlag GmbH & Co. KGaA, Weinheim